Properties of the 120,000- and 95,000-dalton Actin-binding Proteins from *Dictyostelium discoideum* and Their Possible Functions in Assembling the Cytoplasmic Matrix

JOHN CONDEELIS, MARYANNE VAHEY, JOAN M. CARBONI, JAN DEMEY,* and SATOSHI OGIHARA

*Department of Anatomy, Albert Einstein College of Medicine, Bronx, New York 10461, and *Laboratory of Oncology, Janssen Pharmaceutica Laboratories, B-2340 Beerse, Belgium. Dr. Vahey's present address is National Heart, Lung and Blood Institute, Laboratory of Molecular Cardiology, National Institutes of Health, Bethesda, Maryland 20205.*

ABSTRACT The cell cortex of *Dictyostelium* amebae contains an actin-rich cytoplasmic matrix. Changes in geometry of this matrix are believed to regulate protrusive activity and motility of the cell cortex. Two actin-binding proteins (120,000 and 95,000 daltons [120K and 95K]) are present in the cell cortex, and their properties, many of which are described here for the first time, suggest that they regulate growth and organization of cortical microfilaments. The 120K protein is a flexible dimer 35 nm in length with a native molecular mass of 241,000. It nucleates the polymerization of actin and crosslinks the filaments to form branched networks like those seen in situ in the cell cortex. The production of a branched network of short crosslinked filaments results in a lattice that would theoretically generate the maximum rigidity with minimum amount of polymer. This sort of lattice would be very useful as a space-filling cytoskeleton capable of resisting deformation. The 120K protein inhibits the actin-stimulated Mg ATPase of myosin. Competition for actin binding between 120K and myosin, the impenetrability of the 120K-actin network to myosin, and the rigidity of actin filaments that are crosslinked by 120K could all contribute to the decrease in the actin-stimulated Mg ATPase of myosin. The properties of 120K are consistent with a role for this protein in regulating the site of actin filament growth and gelation in the cell but not the assembly of actin-containing structures that would participate in force generation by a sliding-filament mechanism involving myosin. The 95K protein is a rigid dimer 40 nm in length with a native molecular mass of between 190,000 and 210,000. Its physical and antigenic properties lead us to conclude that the 95K protein is *Dictyostelium* α-actinin. Unlike 120K, it crosslinks actin filaments into lateral arrays and increases the actin-stimulated Mg ATPase of myosin. Both activities are regulated by Ca^{2+}. The properties of 95K are consistent with a role in organizing actin filaments in the cell into lateral arrays that are capable of efficient interaction with myosin to produce force for cell motility.

The cytoplasmic matrix is a pervasive filamentous network in the cytoplasm of many eukaryotic cells. This structure was first described by Wolosewick and Porter (42) as a microtrabecular lattice of heterogeneous morphology containing all three of the major filament classes (microfilaments, intermediate filaments, and microtubules) crosslinked to each other by narrow "trabeculae." Recently, workers in many laboratories have begun to study the molecular composition of the cytoplasmic matrix, resolving zones rich in actin, tubulin, and intermediate filament proteins. Some of the individual molecules responsible for growth and crosslinking of filaments in these three zones have been identified. In addition, these studies have shown that there are proteins that mediate the interaction between microtubules and microfilaments and

THE JOURNAL OF CELL BIOLOGY · VOLUME 99 NO. 1 PT. 2 JULY 1984 119s–126s

microfilaments and membranes, further emphasizing the view of the cytoplasm as a mechanically integrated network. These studies are largely summarized in the papers of this supplement.

We have been studying the actin-rich zones of the cytomatrix in ameboid cells. In vegetative amebae of *Dictyostelium discoideum* this zone is found in the cell cortex. The cytoplasmic matrix in the cortex is heterogeneous, being composed of microfilament networks and bundles. Numerous microfilament-membrane contacts are present (11). We are particularly interested in the mechanisms governing assembly of the various actin-containing structures in the cell cortex and the functional consequences of these structures.

Two major actin-binding proteins found in the cell cortex are the 120,000-dalton (120K)[1] (8) and 95,000-dalton (95K) proteins (9, 15), named according to their migration upon SDS polyacrylamide gel electrophoresis (PAGE). Each of these proteins, when mixed with actin, forms an actin-containing structure in vitro with distinct properties. In this paper we detail the properties of both actin-binding proteins and from this derive hypotheses for how each of these proteins assembles an actin-containing cytoplasmic matrix with distinct structure and function.

MATERIALS AND METHODS

Protein Purification: The 120K and 95K proteins were isolated from vegetative amebae of *Dictyostelium discoideum* strain Ax-3 as described (8, 9). Rabbit skeletal muscle myosin was prepared by the method of Kielley and Harrington (23). Rabbit skeletal muscle actin was isolated from an acetone powder by the method of Spudich and Watt (36). Actin used in viscosity studies was further purified by gel filtration on a 1.5 × 70-cm column of Sephacryl S-200 equilibrated and eluted in 5 mM Tris-HCl, pH 7.8, 0.2 mM ATP, 0.5 mM DTT, and 0.1 mM $CaCl_2$. The chicken gizzard α-actinin used in hydrodynamic, viscosity, and ATPase measurements was the gift of M. Titus, Brandeis University, who prepared it according to the method of Feramisco and Burridge (16). Anti-chicken gizzard α-actinin was prepared in rabbits, affinity purified, and used in immunoblots as described (14). The chicken gizzard α-actinin used to prepare antibodies was the gift of J. V. Small, Institute of Molecular Biology, Salzburg, Austria.

SDS-PAGE and Protein Determination: Electrophoresis was carried out according to the method of Laemmli (25). Covalent crosslinking with dimethyl suberimidate was performed by the method of Davies and Stark (12). The amounts of 120K and 95K present in vegetative amebae were determined by quantitative densitometry with a Gilford spectrophotometer as described by Gorovsky et al. (18). Protein concentration was determined according to Lowry et al. (26), and $A_{280}^{1\%}$ was calculated according to Finlayson (17).

ATPase Assay: ATPase activity was assayed by a modification (see reference 31) of the method of Martin and Doty. Incubations were carried out at 27°C with time points taken at 0, 2, 6, and 15 min.

The final ionic conditions were as follows: 30 mM KCl, 1 mM Mg^{2+} ATP, 20 mM PIPES, pH 7.0, 1 mM EGTA, and either 1 mM $CaCl_2$, (pCa 4) or 0.1 mM $CaCl_2$ (pCa 7). The final protein concentrations were 0.006 mg/ml myosin, 0.055 mg/ml F-actin, and 0.055 mg/ml α-actinin, 95K, or 120K (molar ratio of myosin:actin:actin-binding protein = ~0.05:5.0:1.0). These molar ratios of actin-binding protein to actin were chosen to ensure that the gel composed of 120K and actin contained a dense network of filaments (11) and that 95K bundled the actin filaments (9).

The assay mix was assembled without myosin and Mg^{2+} ATP and was incubated at 27°C for 15 min, allowing the F-actin and the actin-binding protein to interact. After 15 min, myosin was added to the mix. The ATPase reaction was started immediately by the addition of Mg^{2+} ATP. In assays in which the 95K was allowed to interact with F-actin at pCa 7 and then exposed to pCa 4, the myosin was added in a buffer containing enough $CaCl_2$ to give a final pCa of 4. All additions were done in such a way that the pH was maintained at 7.0.

Viscometric Assays: Falling-ball viscometry was performed according to the method of MacLean-Fletcher and Pollard (27) at an angle of 45°. Molar ratios were calculated on the basis of native molecular weights for the actin-binding proteins shown in Table II. Details of the assay conditions are given in the legend to Fig. 5.

Determination of Physical Constants: The Stoke's radius was determined by the method of Siegel and Monty (34) by gel filtration on a 1 × 60-cm column of Bio-Rad A 15 M (100–200 mesh) (Bio-Rad Laboratories, Richmond, CA) in 0.6 M KCl, 10 mM PIPES, pH 6.8, 2 mM EGTA, and 2 mM $CaCl_2$. The K_{av} was calculated by: $K_{av} = (V_e - V_0)/(V_t - V_0)$, where V_e is the elution volume, V_0 is the void volume, and V_t is the total volume. The K_{av} of unknowns was compared with the K_{av} of proteins of known Stoke's radii.

The sedimentation coefficient (S 20_w) was determined by the procedure of Martin and Ames (28) using 5 ml gradients of from 5 to 20% sucrose in 0.6 M KCl, 10 mM PIPES, pH 6.8, 2 mM EGTA, and 2 mM $CaCl_2$. The gradients were loaded with 0.1 ml of a mixture of a protein of known S 20_w (0.1 mg/ml catalase) and 0.25 mg/ml of the actin-binding protein. Centrifugation was carried out in a SW-20 rotor at 4°C for 3 h at 100,000 *g*. After fractionation of the gradient the S 20_w of the actin-binding proteins was calculated using catalase as an intrinsic marker. The gradients were calibrated with bovine serum albumin, catalase, and α-actinin.

The diffusion constant (D 20_w), frictional ratio (f/f_0), and native molecular weight (M) were calculated as follows using the determined S 20_w, Stoke's radius (a), and a partial specific volume calculated from the amino acid composition shown in Table I: $M = 6\pi NaS/(1 - vp)$; $D\ 20_w = KT/6\pi na$; $f/f_0 = a/(3vM/4\pi N)^{1/3}$ where n is the viscosity of buffer, N is Avogadro's number, p is the density of buffer, K is Boltzmann's constant, T is absolute temperature, and v is the partial specific volume.

Amino Acid Analysis: The 120K protein was dialyzed against two 4-l changes of 0.5 M acetic acid and then exhaustively against water. The protein was lyophilized to dryness. The more labile 95K protein was rapidly desalted on a Sephadex G 25 column equilibrated in 20 mM sodium bicarbonate, pH 7.0. The desalted protein was lyophilized, resuspended in water, and relyophilized. Cycles of lyophilization and resuspension in water were repeated four times. All samples were hydrolyzed *in vacuo* at 110°C in 6 N HCl, 0.1% phenol for 24 and 96 h and for 24 h after performic acid oxidation. Amino acid analyses were performed with a Glenco Scientific, Inc. (Houston, TX) AV-100 update of a Beckman 120 B amino acid analyzer equipped with a Spectra Physics Inc. (Mountain View, CA) System I computing integrator using standard single column methodology.

Electron Microscopy: Proteins were rotary shadowed in 50% glycerol at an angle of 8° and 4° according to the method of Tyler and Branton (40). The final concentration of protein used in the rotary shadowing experiments on individual proteins was 40 μg/ml. For these studies, proteins were dialyzed into 2 mM Tris-HCl, pH 6.8, 2 mM PIPES, 2 mM EGTA, and 0.1 mM $CaCl_2$. Each histogram is based on analysis of 150 measurements made with a micrometer from prints at a magnification of 59,600.

RESULTS

Physical Properties of the Actin-binding Proteins

The amino acid composition and physical properties of 120K, 95K, and α-actinin are summarized in Tables I and II.[2] The hydrodynamic properties predict that 120K, 95K, and chicken gizzard α-actinin are stable dimers with elongate shapes. These predictions are supported by chemical crosslinking experiments for 120K (Fig. 1) and for 95K as reported elsewhere (9, 15) and the rotary shadowing experiments shown in Figs. 2 and 3.

Rotary shadowing is particularly useful for determining the size, shape, flexibility (degrees of freedom of bending), and topography of proteins. Fig. 2 compares 120K, 95K, and chicken gizzard α-actinin at high and low angles of shadow. High angles of shadow result in sharp definition of the proteins resulting in preparations suitable for size measurements (Fig. 2, *a*, *c*, and *e*). The measurements shown in Fig. 3 were made from preparations like these. Lower angles of shadow (Fig. 2,

[1] *Abbreviations used in this paper:* 95K, 95,000-dalton actin-binding protein, 120K, 120,000-dalton actin-binding protein; GAR-PAP, goat anti-rabbit-peroxidase–anti-peroxidase; HMM, heavy meromyosin; PAGE, polyacrylamide gel electrophoresis.

[2] All of the results in Figs. 1; 2, *a*, *b*, *e*, and *f*; 3, *b* and *c*; 4; and 6 and Table I are reported here for the first time. The properties summarized in Table II for 120K, 95K, and chicken-gizzard α-actinin are reported here for the first time except where indicated by footnotes.

b, *d*, and *f*) reveal surface detail in the protein that may be related to subunit composition and polypeptide conformation. In sum, Figs. 2 and 3 show that 120K is a flexible rod 35 nm in length with several globular domains, whereas both 95K and chicken gizzard α-actinin are more rigid rods about 40 nm in length with an open, two-stranded appearance at low shadow angles. We (9) have previously presented similar data for 95K. It is repeated here for comparison with chicken gizzard α-actinin to demonstrate that the two proteins are indistinguishable by this technique.

To further investigate the possibility that 95K is an α-actinin, we tested the ability of antibodies against chicken gizzard α-actinin to cross-react with 95K in western blots. As shown in Fig. 4, anti-α-actinin reacts specifically with 95K in blots of whole *Dictyostelium* amebae and with blots of purified 95K.

TABLE I

Amino Acid Composition of 120K, 95K, and Rabbit Skeletal Muscle α-Actinin

Amino acid	α-Actinin	95K	120K
His	26.2	17.1	30.4
Lys	53.9	64.2	32.4
Arg	68.2	37.2	20.3
Asp	108.4	100.2	82.7
Thr	29.6	57.5*	52.8*
Ser	49.3	85.3*	160.6*
Glu	164.2	190.1	150.0
Pro	46.7	46.2	49.9
Gly	62.5	117.7	200.5
Ala	96.7	77.0	100.5
½Cys	ND	ND	4.7§
Val	44.7	40.3‡	51.4‡
Meth	ND	ND	6.9§
Ile	47.7	41.7‡	28.1‡
Leu	107.7	71.5	38.9
Tyr	26.6	18.5	19.1
Phe	35.4	34.7	19.6

Values for α-actinin are those of Robson et al. (32) for purified rabbit skeletal muscle α-actinin. The figures given are residues of amino acid per 1,000 residues. ND, not determined.
* Normalized by extrapolation to zero time hydrolysis.
‡ Values obtained after 96-h hydrolysis.
§ Determined after performic acid oxidation.

Functional Properties of the Actin-binding Proteins

α-Actinin, 120K, and 95K are all capable of increasing the viscosity of actin solutions, and this has been shown to result from the crosslinking of actin filaments (8, 9, 11, 30). However, there are important differences in the actin-binding and crosslinking activities of these proteins. First, although muscle and nonmuscle α-actinins appear to have approximately the same actin crosslinking activity in vitro (2, 24), the nonmuscle α-actinins, including *Dictyostelium* 95K, are inhibited from crosslinking by calcium (2, 9, 15). Second, as shown in Fig. 5, 120K protein is approximately five times more potent than 95K protein on a molar basis in increasing the low shear viscosity of actin when both proteins are assayed under iden-

TABLE II

Properties of 120K, 95K, and α-Actinin

	120K	95K	Chicken gizzard α-actinin*	Rabbit skeletal muscle α-actinin‡
Content in whole cell	2.3%	1.9%	—	1%
Subunits	2	2	2	2
Partial specific volume§	0.70	0.72	—	0.73
Stoke's radius	8.6 nm	7.3 (7.4) nm‖	7.7	7.7
S 20_w (10^{-13} s)	7.4	7.1	6.6	6.2
Molecular mass (SDS PAGE)	120,000	95,000	100,000	100,000
Molecular mass (native)	241,000	210,000¶	214,000	196,000–210,000
$A^{1\%}_{278}$	—	—	—	9.7
$A^{1\%}_{280}$	5.9	7.7	—	—
Contour length	35 nm	40 nm	41 nm	40 nm
f/f_0	2.10	1.87	1.94	1.98
D 20_w (10^{-7} cm^2 s^{-1})	2.49	2.95	2.79	2.71
Antigenic cross-reactivity	None**	Skeletal muscle α-actinin‡‡	Skeletal muscle α-actinin, 95K	—
Effect on Mg ATPase of actomyosin	X0.6	X0, +Ca^{2+} X2.6, −Ca^{2+} X4, −Ca^{2+} then +Ca^{2+}	X2.5, ±Ca^{2+}	X1.3-2, ±Ca^{2+}
Actin structure formed	Meshwork§§	Lateral array‖‖	—	Lateral array¶

All properties of 120K, 95K, and chicken gizzard α-actinin shown here were measured as described in Materials and Methods except molecular mass (native), f/f_0, and D 20_w. These were calculated according to the equations in Materials and Methods.
* Values for chicken gizzard α-actinin determined by us as described in Materials and Methods.
‡ All values for rabbit skeletal muscle α-actinin from references 1, 32, and 39.
§ Calculated from the amino acid composition given in Table I according to Schachman (33).
‖ Stoke's radius of 7.4 from Fechheimer et al. (15).
¶ From Podlubnaya et al. (30).
** None against 95K, actin, α-actinin, or *Dictyostelium* myosin.
‡‡ Carboni, J. M., and J. Condeelis, manuscript in preparation.
§§ From Condeelis (11).
‖‖ From Condeelis and Vahey (9).
¶¶ Values for molecular mass determined previously by chemical crosslinking are 190,000 (9) and 200,000–250,000 (15).

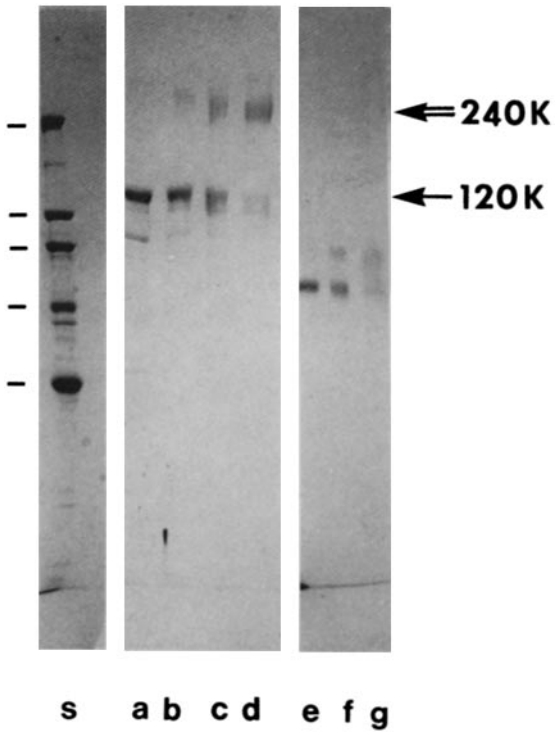

FIGURE 1 SDS PAGE of dimethyl suberimidate crosslinking of the 120K protein. Conditions were 0.2 mg/ml protein in 0.2 M triethanolamine, pH 8.5, and 1 mg/ml dimethyl suberimidate. The reaction was allowed to proceed for (a, e) 0 min, (*b*) 1 h, (c, *f*) 3 h, and (*d*, *g*) 12 h. *a–d* show the 120K protein, and e–g show bovine serum albumin. The 120K protein (arrow) is crosslinked to a species measuring 240,000 daltons (double arrow) whereas BSA retains its monomeric molecular weight. Samples were run on a 5–20% gradient slab gel. Standards (*s*) were myosin (200,000), β-galactosidase (116,250), phosphorylase *b* (92,000), bovine serum albumin (66,200), and ovalbumin (45,000).

tical conditions. Furthermore, the crosslinking activity of 120K does not exhibit sensitivity to calcium.

Another functional difference among these proteins is their effect on the actin stimulated Mg ATPase of myosin thick filaments at physiologic ionic strength. It has been shown (24) that rabbit skeletal muscle (1, 32), chicken gizzard, and porcine kidney α-actinin increase the actin-stimulated Mg ATPase of myosin by about twofold. As shown in Fig. 6, *Dictyostelium* 95K shows a similar enhancement of the Mg ATPase, but this effect is calcium regulated.

Under conditions in which the 95K protein does not bind to actin (pCa 4) (9), 95K protein had no effect on the actomyosin ATPase activity. Alternatively, at pCa 7, conditions under which the binding of 95K protein to F-actinin is optimal (9), there is a 2.6-fold enhancement of the Mg^{2+} ATPase activity of actomyosin in the presence of 95K protein. A similar stimulation of the Mg^{2+} ATPase of actomyosin occurred in the presence of chicken gizzard α-actinin under our assay conditions. However, unlike the case with 95K protein, this stimulation was not inhibited at pCa 4 (Fig. 6).

In additional experiments, 95K protein was allowed to interact with actomyosin under conditions (pCa 7) that promote its binding to and bundling of F-actin, and then the Mg^{2+} ATPase was assayed under conditions (pCa 4) that cause 95K protein to dissociate from actin (9). Here, there was a fourfold enhancement of the Mg^{2+} ATPase activity of actomyosin in the presence of 95K protein. Control experiments demonstrated that neither 95K protein nor α-actinin exhibits an inherent ATPase activity and that they have no effect on myosin ATPase in the absence of actin.

Also shown in Fig. 6 is the effect of 120K on the actin-stimulated Mg ATPase of myosin thick filaments. Under the same assay conditions as those used for α-actinin and 95K, the 120K caused an inhibition in the ATPase activity. Similar results were obtained when *Dictyostelium* myosin thick filaments were substituted for rabbit skeletal muscle myosin thick filaments. This is consistent with the 120K inhibition of the actin-stimulated Mg ATPase of heavy meromyosin (HMM) reported previously (8).

DISCUSSION

Properties of 120K and Dictyostelium *α-Actinin*

The 120K and 95K actin-binding proteins are structurally and functionally distinct molecules. They differ in their physical properties (Table II, Figs. 2 and 3), ability to increase the apparent viscosity of actin (Fig. 5), the morphology of structures formed with actin in vitro (9, 11), sensitivity to Ca^{2+}, effect on the ability of F-actin to stimulate the Mg^{2+} ATPase of myosin (Fig. 6), two-dimensional peptide maps (15), and immunological cross-reactivity (Fig. 4 and reference 7).

However, α-actinins from rabbit skeletal muscle and chicken gizzard have sizes and shapes that are very similar to those of *Dictyostelium* 95K (Table II, Figs. 2 and 3), and all stimulate the Mg^{2+} ATPase of synthetic actomyosin (1, 24). Furthermore, chicken gizzard α-actinin and 95K share antigenic cross-reactivity. On the basis of these results we conclude that 95K is *Dictyostelium* α-actinin.

The 120K protein is a rod-shaped dimer that nucleates polymerization of actin (11), crosslinks actin filaments to form branched networks of filaments (6, 11) and inhibits the actin-activated Mg^{2+} ATPase of myosin thick filaments and HMM (8). The effects of 120K protein on the growth and structure of actin filaments are similar to those reported for macrophage actin-binding protein (20). The inhibitory effect of 120K protein on the actin-activated Mg^{2+} ATPase of myosin is similar to that reported for chicken gizzard filamin (13). However, the 120K protein is not easily categorized as a filaminlike protein. Both filamin and macrophage actin-binding protein are large molecules with subunits in excess of 250,000 daltons and native molecular weights greater than 500,000 (19, 41). These proteins are long, flexible dimers more than 160 nm in length and have similar amino acid compositions (35, 37). On the other hand, the 120K protein is a more compact rod with a native molecular weight of 241,000. Furthermore, the amino acid composition of 120K protein differs substantially from those of filamin and macrophage actin-binding protein (35, 37).

That filamin, macrophage actin-binding protein, and 120K protein exhibit similar functions in vitro but are structurally distinct suggests that some of the properties of filaminlike proteins, such as the long, flexible conformation exhibited in vitro, may not be essential to promote near perpendicular crosslinks between actin filaments, because the 120K protein also produces these types of crosslinks but is a more compact rod (11, 19).

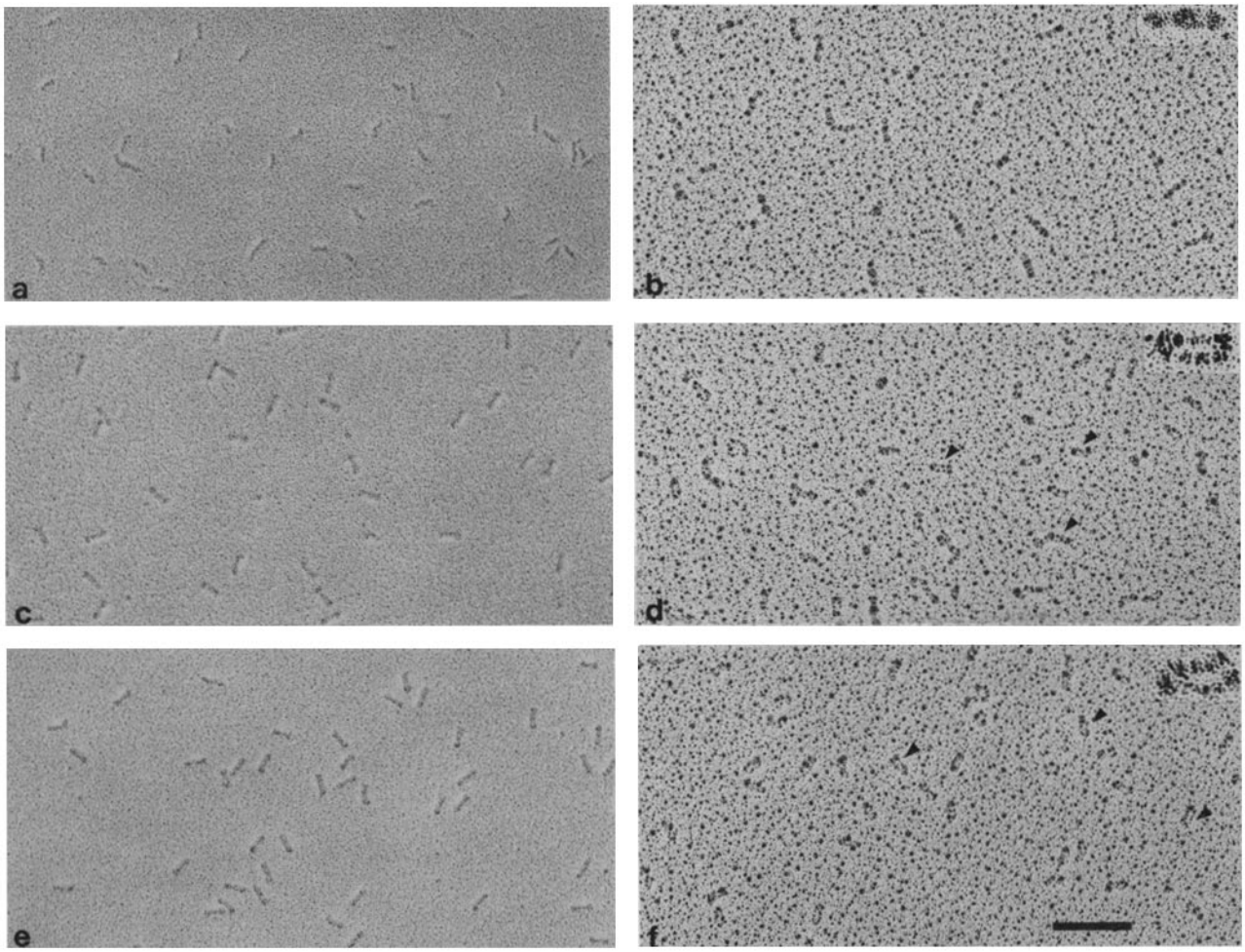

FIGURE 2 Electron micrographs of 120K, 95K, and α-actinin after rotary shadowing with platinum. Shadowing at 8° (*a*, *c*, *e*) gives the protein a sharp outline while shadowing at 4° (*b*, *d*, *f*) reveals subunit packing. (*a*, *b*) 120K protein is a rod with several globular domains per molecule. Some of these rods are bent, presumably by the preparation techniques indicating their flexibility. (*c*, *d*) 95K protein is a rigid rod with two discernible strands packed side by side. Presumably these are the two subunits of the molecule. (*e*, *f*) Chicken gizzard α-actinin is indistinguishable from 95K in rotary shadowing. Arrowheads in *d* and *f* indicate molecules in which two strands can be visualized. × 75,000. Bar, 160 μm. *Insets* show a molecule of each type at a higher magnification after shadowing at 4°. × 268,000.

Possible Functions of 120K and α-Actinin in the Cytomatrix

120K PROTEIN: The ability of 120K protein to nucleate actin polymerization and crosslink F-actin into networks of branched filaments (11) suggests an explanation for its greater efficiency in gelling actin as compared to α-actinin or HMM (8). The production of a branched network of short cross-linked filaments results in a structure having the maximum rigidity with the minimum amount of polymer (reviewed in reference 38). This sort of structure would be very useful as a space-filling cytoskeleton capable of resisting deformation. Such actin-containing networks are seen in areas of the cell cortex in *Dictyostelium* amebae that are rich in 120K (3, 7, 10, 11, 29).

A property of 120K that may be important in vivo is its inhibition of the actin-stimulated Mg ATPase of myosin. Inhibition cannot be accounted for by an interaction between 120K and ATP or myosin. That is, 120K exhibits neither an ATPase activity nor a kinase activity toward itself or myosin (Ogihara, S., and J. Condeelis, unpublished data), and 120K has no effect on the Mg ATPase of myosin in the absence of actin (8).

There are several possible explanations for this inhibition:

1. 120K competes for actin-binding with myosin. This is the simplest explanation for the inhibition and it is consistent with the increased inhibition of the Mg ATPase of acto-HMM observed with increasing molar ratios of 120K:actin (8).
2. Large molecules such as HMM, myosin, and myosin oligomers cannot penetrate the 120K-actin gel. This causes a decrease in the amount of actin that is accessible for binding to myosin and, therefore, a drop in the Mg ATPase activity. This possibility is consistent with measurements made of the filament density in 120K-actin gels by stereo electron microscopy (11). These measurements demonstrate that the pore size of the gel decreases as the molar ratio of 120K:actin increases. The pore size is measured as the average filament length between filament cross-over points in the gel. For example, at a molar ratio of 1:14 the pore size ranges from 24 to 56 nm (11). A myosin monomer 150 nm in length would diffuse very slowly through such a lattice, whereas oligomers of myosin would become trapped (Fig. 7).

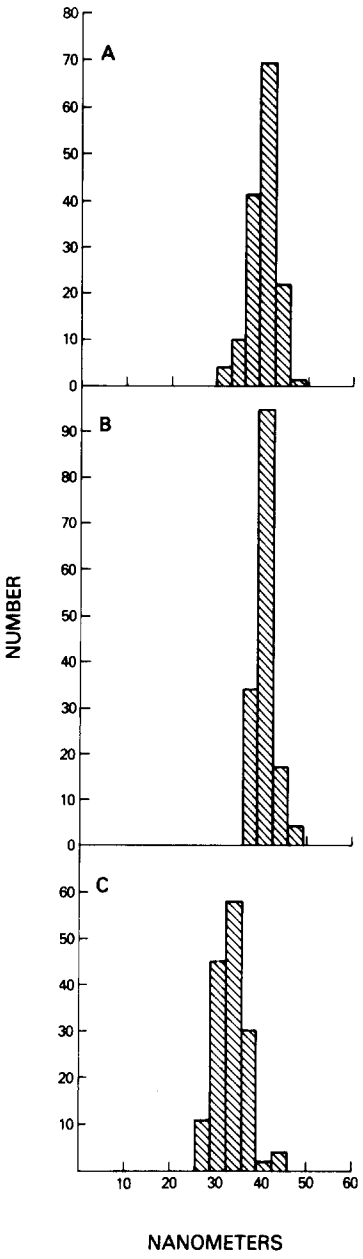

FIGURE 3 Length histograms of the actin-binding proteins shadowed at 8°. The 95K protein (*A*) and α-actinin (*B*) have very similar length distributions, measuring 40.4 ± 2.7 and 41.1 ± 1.8 nm, respectively. The 120K protein (*C*) is shorter, with an average length of 34.9 ± 3.0 nm.

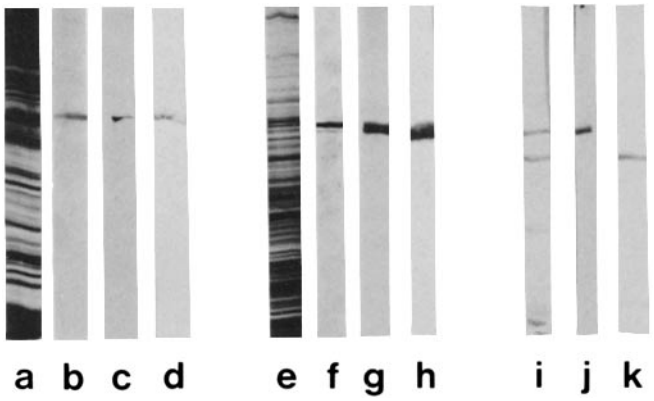

FIGURE 4 SDS PAGE and nitrocellulose blots of (*a*, *b*) whole gizzard, (*c*, *d*) α-actinin, (*e*, *f*, *i*, *k*) homogenate of *Dictyostelium* amebae, (*g*, *h*, *j*) 95K. *a*, *c*, *e*, and *g* are SDS PAGE stained with Coomassie Blue. *b*, *d*, *i*, and *j* are blots reacted with anti-α-actinin followed by goat anti-rabbit-peroxidase–anti-peroxidase (GAR-PAP). *f* and *h* are blots reacted with anti-95K followed by GAR-PAP. *k* is a blot reacted with buffer only followed by GAR-PAP. *a–d* establish the monospecificity of anti-α-actinin. *e–h* establish the monospecificity of anti-95K. *i* and *k* establish that anti-α-actinin stains only one band in whole *Dictyostelium* homogenates, i.e., the same band stained by anti-95K. Lower band in *i* is due to the secondary antibody as demonstrated in *k*. *j* shows that anti-α-actinin also stains purified 95K.

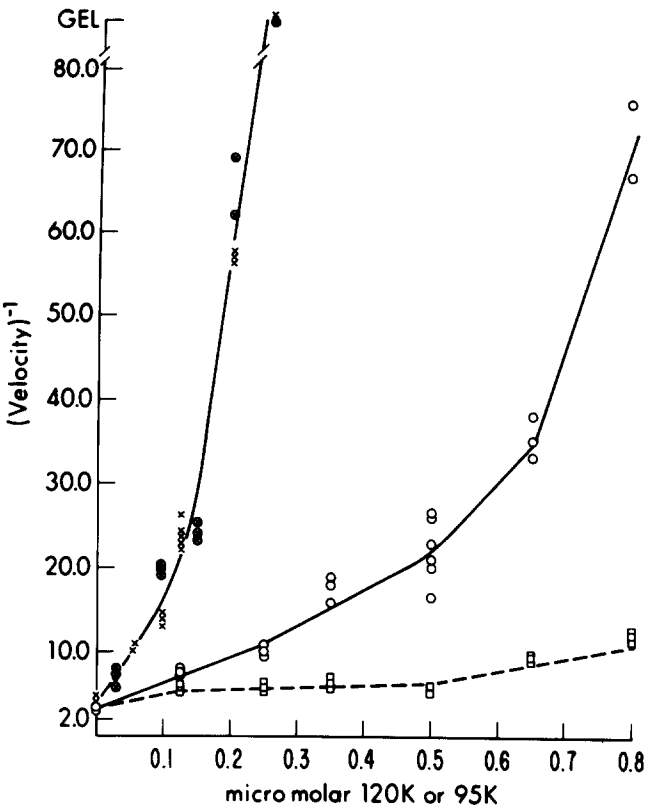

FIGURE 5 Rabbit muscle actin at a concentration of 19 μM was polymerized in the presence of either 120K protein or 95K protein for 18 min at 22°C in 20 mM KCl, 2 mM $MgSO_4$, 5 mM PIPES, 2 mM EGTA, pH 7.0, with the concentration of $CaCl_2$ indicated below. Measurements were made at an angle of 45°. (×) 120K protein with 0.1 mM $CaCl_2$. (⊗) 120K protein with 2.0 mM $CaCl_2$. (○) 95K protein with 0.1 mM $CaCl_2$. (□) 95K protein with 2.0 mM $CaCl_2$. Concentrations of actin-binding proteins were calculated from the native molecular weights for 120K protein and 95K protein shown in Table II.

3. Actin filaments in a 120K-actin lattice are randomly oriented and are unable to slide due to the 120K crosslinks. Hence, myosin oligomers that are trapped within the 120K-actin lattice cannot recruit actin filaments around themselves as occurs in the A band of striated muscle during contraction. This would reduce the amount of actin that is accessible to myosin and, thereby, lower the Mg ATPase activity of myosin (Fig. 7). As yet there are no data to support this last hypothesis.

A potentially important property of 120K protein is its ability to nucleate actin polymerization (11). This property is correlated with the fact the 120K protein decreases the critical concentration of actin at steady-state (8). The localization of 120K protein in the cortex of *Dictyostelium* amebae by immunofluorescence (3, 7) and immunogold electron microscopy (29) suggests that 120K protein may function as a nucleation site for actin filament growth to produce extension of the cortex during ameboid movement. In this scheme, actin polymerization occurs from 120K protein in the cytoplasm and proceeds toward the cell membrane with the faster

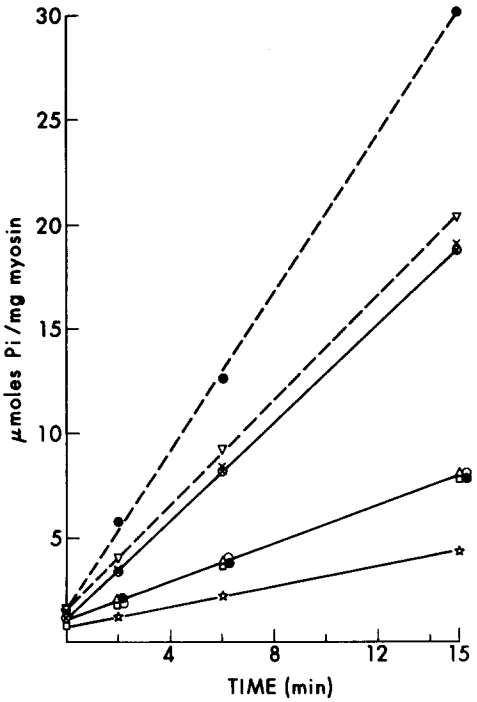

FIGURE 6 Effect of 95K protein, α-actinin, and 120K protein on the F-actin-stimulated Mg ATPase activity of myosin thick filaments at physiologic ionic strength. Actomyosin alone at pCa 4, ●——●; pCa 7, ○; pCa 7 followed by pCa4, △. α-Actinin plus actomyosin at pCa4, ×; pCa7, ⊗. 95K protein plus actomyosin at pCa4, □; pCa7, ▽; pCa7 followed by pCa4, ●---●. 120K protein plus actomyosin at pCa7, ★.

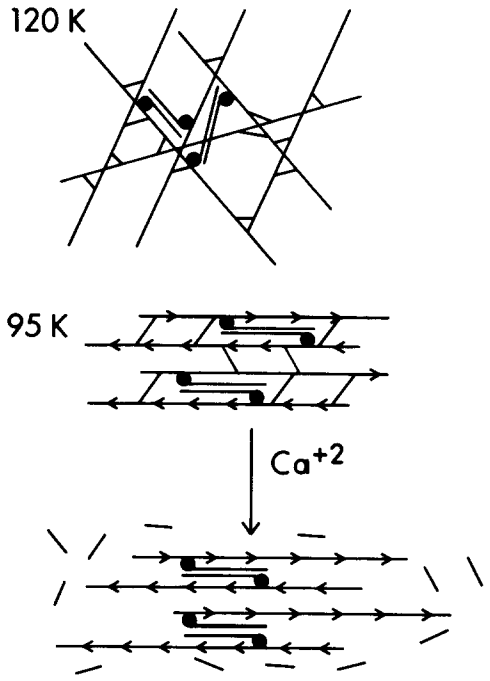

FIGURE 7 Schematic (not drawn to scale) of the types of structures formed from F-actin in the presence of 120K and 95K and how they might affect motility resulting from a sliding-filament type of interaction between actin and myosin. (*Top*) The 120K protein (short rods) crosslinks actin filaments (longer lines) to form a network the density of which increases with the molar ratio of 120K:actin. Competition for actin binding between 120K and myosin (lines connected to filled circles), the impenetrability of the network to myosin, and the rigidity of crosslinked actin filaments could all contribute to the decrease in the actin-stimulated Mg ATPase of myosin observed in the presence of 120K. (*Bottom*) The 95K protein (short rods) crosslinks actin filaments (longer lines) to form loose lateral arrays. This might increase the local concentration of F-actin that is available for binding to myosin. Penetration of these lateral arrays of filaments by myosin (lines connected to filled circles) might be facilitated by the length and rigidity of the 95K cross-bridges separating adjacent actin filaments as well as the Ca^{2+}-induced loss of crosslinks. All of these factors might contribute to the Ca^{2+}-sensitive stimulation of the Mg ATPase of actomyosin observed in the presence of 95K.

growing barbed ends of actin filaments approaching the cytoplasmic surface of the cell membrane. The resulting filaments could then dock at various sites on the membrane to achieve lateral and barbed-end attachments. Because 120K protein would also crosslink the newly grown filaments, they would become linked to the cortical actin network to form an expanding gel. The implications of this sort of arrangement have been discussed (11).

In summary, the properties of 120K are consistent with a role for this protein in regulating the site of actin filament growth and gelation. The resulting lattice of 120K and actin would resist the generation of motility by a sliding-filament mechanism involving myosin.

To further evaluate this hypothesis for the function of 120K protein more information is necessary about the location of this protein in the cell (29) and how its interaction with actin is regulated.

α-ACTININ: A property that is considered to be diagnostic for α-actinin is the ability to stimulate the Mg ATPase of isolated actomyosin at physiologic ionic strength (1, 24). The significance of this property for the function of α-actinin in vivo is not clear because the molecular mechanism underlying it remains unknown. Two working hypotheses for the mechanism of stimulation of the Mg ATPase of actomyosin by α-actinin follow:

1. α-Actinin, unlike 120K, tends to crosslink actin filaments into lateral arrays that occupy less volume than the original random network of filaments (Fig. 7). This would increase the local concentration of actin filaments, thereby increasing the actin-stimulated Mg ATPase of myosin. This possibility is consistent with the ability of α-actinin to induce actin filaments to form loose lateral arrays in vitro (9, 22, 30).

2. α-Actinins are rigid rods about 40 nm in length. Actin filaments, when crosslinked by α-actinin, would be spaced at intervals of ~40 nm, thereby providing a space through which myosin and myosin oligomers could penetrate the lateral array in a direction parallel to the actin filaments. Because the crosslinks are Ca^{2+} labile, subsequent addition of Ca^{2+} might further increase the efficiency of penetration by myosin (Fig. 7). In both cases, the increased accessibility of actin to myosin would be reflected by an increased Mg ATPase, as is shown in Fig. 6.

In summary, we hypothesize that the function of 95K protein and other nonmuscle α-actinins is to organize actin filaments in the cytoplasmic matrix into lateral arrays capable of efficient interaction with myosin to produce force for cell motility. The pCa- and pH-dependent regulation of crosslinking by 95K and other nonmuscle α-actinins suggests a mechanism whereby the cell could determine the location of assembly of these lateral arrays of filaments.

We are most grateful to Dr. Howard Steinman of the Department of

Biochemistry, Albert Einstein College of Medicine, for his help in determining the amino acid composition of the 120K and 95K proteins and to Margaret Titus and Dr. J. V. Small for supplying α-actinin. We would like to thank Mr. Rick S. Hock for his help in preparing rabbit actin. We are thankful for the constructive criticisms given to the manuscript by Ms. Holly Bennett and Drs. Patricia A. Detmers and Larry Tobacman and the typing skills of Ms. Holly Chernin, Edna Horowitz, Chris Hubertus, and Lorraine Letterese.

This work was supported by grant GM 25813 from the National Institutes of Health and the Martin Foundation. J. Condeelis is a Rita Allen Foundation Scholar.

REFERENCES

1. Arakawa, N., R. Robson, and R. Goll. 1970. An improved method for the separation of α-actinin from rabbit striated muscle. *Biochim. Biophys. Acta.* 200:284–295.
2. Burridge, K., and J. Feramisco. 1981. Non-muscle α-actinins are calcium sensitive actin binding proteins. *Nature (Lond.).* 294:565–567.
3. Carboni, J. M., and J. Condeelis. 1983. Ligand induced changes in the structure of the actin cortex. *J. Cell Biol.* 97(2, Pt. 2):269*a*.
4. Condeelis, J. 1980. Reciprocal interactions between the actin lattice and cell membrane. *Neurosci. Res. Program Bull.* 19:83–101.
5. Condeelis, J., and D. Taylor. 1977. Control of gelation, solation, and contraction in extracts from *D. discoideum*. *J. Cell Biol.* 97:901–927.
6. Condeelis, J., and J. Wolosewick. 1980. The actin lattice: composition, structure and membrane attachment. *In* 38th Annual Proceedings of the Electron Microscopy Society of America. 420–423.
7. Condeelis, J., J. Salisbury, and K. Fujiwara. 1981. A new protein that gels F-actin in the cell cortex of *D. discoideum*. *Nature (Lond.).* 292:161–163.
8. Condeelis, J., S. Geosits, and M. Vahey. 1982. Isolation of a new actin binding protein from *D. discoideum*. *Cell Motility.* 2:273–285.
9. Condeelis, J., and M. Vahey. 1982. A calcium- and pH-regulated protein from *D. Discoideum* that crosslinks actin filaments. *J. Cell Biol.* 94:466–471.
10. Condeelis, J. 1983. Rheological properties of cytoplasm. Significance for the organization of spatial information and movement. *In* Modern Cell Biology Vol. 2: Spatial Organizatin of Eukaryotic Cells. J. R. McIntosh, editor. Alan R. Liss, Inc., New York. 225.
11. Condeelis, J. 1981. Microfilament-membrane interactions in cell shape and surface architecture. *In* International Cell Biology 1980–81. J. G. Schweiger, editor. Springer-Verlag, Berlin. 306–320.
12. Davies, G., and G. Stark. 1970. Use of dimethyl suberimidate in studying the subunit structure of oligomeric proteins. *Proc. Natl. Acad. Sci. USA.* 66:651–656.
13. Davies, G., P. Betchtel, and I. Pastan. 1977. Filamin inhibits actin activation of heavy meromyosin ATPase. *FEBS (Fed. Eur. Biochem. Soc.) LETT.* 77:228–232.
14. DeMey, J. 1982. Raising and using antibodies for immunocytochemistry. *In* Immunocytochemistry: Applications in Pathology and Biology. J. Polak and S. Van Noorder, editors. Wright and Sons, Ltd., London. 82–112.
15. Fechheimer, M., J. Brier, M. Rockwell, E. Luna, and D. Taylor. 1982. A calcium and pH regulated actin binding protein from *D. discoideum*. *Cell Motility.* 2:287–308.
16. Feramisco, J., and K. Burridge. 1981. A rapid purification of α-actinin, filamin and a 130,000 dalton protein from smooth muscle. *J. Biol. Chem.* 255:1194–1199.
17. Finlayson, J. 1969. Basic Biochemical Calculations. Addison-Wesley Publishing Co., Inc. Reading, MA. 121.
18. Gorovsky, M., K. Carlson, and J. Rosenbaum. 1969. Simple method for quantitative densitometry of polyacrylamide gels using fast green. *Anal. Biochem.* 35:359–370.
19. Hartwig, J., and T. Stossel. 1981. Structure of macrophage actin binding protein molecules in solution and interacting with actin filaments. *J. Mol. Biol.* 145:563–581.
20. Hartwig, J., J. Tyler, and T. Stossel. 1980. Actin-binding proteins promote the bipolar and perpendicular branching of actin filaments. *J. Cell Biol.* 87:841–848.
21. Hellewell, S., and D. Taylor. 1979. The contractile basis of amoeboid movement. VI. The solation-contraction coupling hypothesis. *J. Cell Biol.* 83:633–648.
22. Jockush, B., and G. Isenberg. 1981. Interaction of α-actinin and vinculin with actin: opposite effects on filament network formation. *Proc. Natl. Acad. Sci. USA.* 78:3005–3009.
23. Kielley, J., and D. Harrington. 1960. A model for the myosin molecule. *Biochim. Biophys. Acta.* 41:401–421.
24. Kobayashi, R., and Y. Tashima. 1983. Purification and characterization of an α-actinin-like protein from porcine kidney. *Biochim. Biophys. Acta.* 745:209–216.
25. Laemmli, U. 1970. Cleavage of structural proteins during the assembly of the head of bacteriophage T-4. *Nature (Lond.).* 227:680–685.
26. Lowry, O., N. Rosebrough, A. Farr, and R. Randall. 1951. Protein measurement with the Folin phenol reagent. *J. Biol. Chem.* 193:265–275.
27. MacLean-Fletcher, S., and T. Pollard. 1980. Viscometric analysis of the gelation of *Acanthamoeba* extracts and purification of two gelation factors. *J. Cell Biol.* 85:414–428.
28. Martin, R., and B. Ames. 1961. A method of determining the sedimentation behavior of enzymes: application to protein mixtures. *J. Biol. Chem.* 236:1372–1379.
29. Ogihara, S., and J. Condeelis. 1983. Electron microscopic localization of myosin and 120K actin binding protein in the cortical actin matrix using IgG-gold. *J. Cell Biol.* 97(2, Pt. 2):270*a*. (Abstr.)
30. Podlubnaya, Z., L. Tszhovrebova, M. Zaalishvili, and G. Stefanenko. 1975. Electron microscopic study of α-actinin. *J. Mol. Biol.* 92:357–359.
31. Pollard, T., and E. Korn. 1973. *Acanthamoeba* myosin: isolation from *Acanthamoeba castellanii* of an enzyme similar to muscle myosin. *J. Biol. Chem.* 248:4682–4690.
32. Robson, R., D. Goll, N. Arakawa, and M. Stromer. 1970. Purification and properties of α-actinin from rabbit skeletal muscle. *Biochim. Biophys. Acta.* 200:296–318.
33. Schachman, H. 1952. Ultracentrifugation, diffusion and viscometry. *Methods Enzymol.* 4:70.
34. Siegel, L., and K. Monty. 1966. Determination of molecular weights and frictional ratios of proteins in impure systems by the use of gel filtration and density gradient centrifugation. *Biochim. Biophys. Acta.* 112:346–362.
35. Shizuta, Y., H. Shizuta, M. Gallo, M. Davies, I. Pastan, and M. Lewis. 1976. Purification and properties of filamin, an actin binding protein from chicken gizzard. *J. Biol. Chem.* 251:6562–6567.
36. Spudich, J., and S. Watt. 1971. Biochemical studies of the interaction of tropomyosin-troponin complex with actin and the proteolytic fragments of myosin. *J. Biol. Chem.* 246:4866–4871.
37. Stossel, T., and J. Hartwig. 1976. Interactions of actin, myosin, and new actin-binding protein of rabbit pulmonary macrophages: role in cytoplasmic movement and phagocytosis. *J. Cell Biol.* 68:602–619.
38. Stossel, T. 1983. Spatial organization of cortical cytoplasm in macrophages. *In* Modern Cell Biology Vol. 2: Spatial Organization of Eukaryotic Cells. J. R. McIntosh, editor. Alan R. Liss, Inc. New York. 203.
39. Suzuki, A., D. Goll, I. Singh, R. Allen, R. Robson, and M. Stromer. 1976. Some properties of purified skeletal muscle α-actinin. *J. Biol. Chem.* 251:6860–6870.
40. Tyler, J., and D. Branton. 1980. Rotary shadowing of extended molecules dried from glycerol. *J. Ultrastruct. Res.* 71:95–102.
41. Wang, K. 1977. Filamin, a new high molecular weight protein found in smooth muscle and non-muscle cells. Purification and properties of chicken gizzard filamin. *Biochemistry.* 16:1857–1865.
42. Wolosewick, J., and K. Porter. 1979. Microtrabecular lattice of the cytoplasmic ground substance. Artifact or reality? *J. Cell Biol.* 82:114–139.